JOURNAL OF SOLID STATE CHEMISTRY 39, 387–394 (1981)

NMR Study of Water Reorientation in Molybdic Acids: $MoO_3 \cdot 2H_2O$ and Yellow $MoO_3 \cdot H_2O$

R. H. JARMAN, P. G. DICKENS, AND R. C. T. SLADE*

Inorganic Chemistry Laboratory, University of Oxford, South Parks Road, Oxford OX1 3QR, England

Received January 14, 1981; in revised form May 23, 1981

Proton NMR relaxation times (T_2, T_1, $T_{1\rho}$) are reported for powder samples of $MoO_3 \cdot 2H_2O$ and yellow $MoO_3 \cdot H_2O$ in the temperature range 150–325 K and at 20 and 60 MHz. No translation of hydrogen atoms is detected but the spin-lattice relaxation behavior indicates reorientation of H_2O molecules. The waters coordinated to Mo atoms undergo 180° flips (about their C_2 axes) with similar motional parameters in both compounds. The interlayer waters in $MoO_3 \cdot 2H_2O$ undergo 180° flips with different parameters. An assumed Arrhenius-type temperature dependence of correlation times leads to preexponential factors which are "anomalously" low. The possible involvement of temperature-dependent activation barriers is discussed.

Introduction

The so-called molybdic acids are hydrates of molybdenum trioxide, $MoO_3 \cdot nH_2O$. The yellow dihydrate $MoO_3 \cdot 2H_2O$ and the white and yellow forms of the monohydrate $MoO_3 \cdot H_2O$ are definite phases.

The crystal structure of $MoO_3 \cdot 2H_2O$ has been investigated using single-crystal X-ray techniques (*1*, *2*) and is illustrated in Fig. 1, the hydrogen atoms being omitted for clarity. The basic structural elements are layers of corner-shared MoO_6 octahedra. The water molecules fall into two classes: (a) those between the layers (large circles in Fig. 1) and (b) those coordinated to an Mo atom with the oxygen atom at an apex of the MoO_6 octahedron (small circles). The hydrogen atom positions have been estimated by refinement of single-crystal X-ray data (*1*, *2*). The layers are held together by hydrogen bonds, each coordinated H_2O donating to two interlayer waters and each interlayer H_2O donating one hydrogen to an unshared oxygen in the next layer and the other to a weak bifurcated bond to a coordinated H_2O and an oxygen shared between octahedra.

A structural model for the yellow monohydrate $MoO_3 \cdot H_2O$ has been proposed after the observation that the first-stage dehydration of the dihydrate is strongly topotactic (*3*). The structure is said to consist of layers of $MoO_5(OH_2)$ octahedra sharing corners and held together by hydrogen bonds; i.e., the interlayer waters in Fig. 1 are lost on dehydration of the dihydrate to give the yellow monohydrate.

NMR and ir studies preceded crystallographic studies in establishing the presence

* Address correspondence to this author at his permanent address: Department of Chemistry, University of Exeter, Stocker Road, Exeter EX4 4QD, England.

0022-4596/81/120387-08$02.00/0

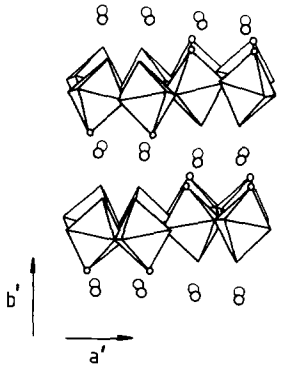

FIG. 1. The structure of $MoO_3 \cdot 2H_2O$. Interlayer waters are represented by large circles and coordinated waters by small circles. The axis system shown (after Krebs (*2*)) is related to that of Lindquist (*7*) by $\mathbf{a}' = \frac{1}{2}(\mathbf{a} + 2\mathbf{c})$ and $\mathbf{b}' = 2\mathbf{b}$.

of water molecules in the molybdic acids (*4*). In the present work we have used measurements of ^1H NMR relaxation times of powder samples to investigate the reorientations of the water molecules in crystalline $MoO_3 \cdot 2H_2O$ and yellow $MoO_3 \cdot H_2O$.

Materials

Yellow molybdic acid $MoO_3 \cdot 2H_2O$ was prepared following Freedman (*5*). 50 g of sodium molybdate was dissolved in 100 cm^3 of water and added to 300 cm^3 of 5 *M* aqueous nitric acid at room temperature and then allowed to stand for several weeks. The precipitate of $MoO_3 \cdot 2H_2O$ was collected, washed with aqueous nitric acid followed by water and air dried at 20°C.

The yellow monohydrate $MoO_3 \cdot H_2O$ was prepared by controlled heating of $MoO_3 \cdot 2H_2O$ at 50°C until sufficient water loss was achieved.

Thermogravimetric dehydration of the products gave the formulae $MoO_3 \cdot 1.99\ H_2O$ and $MoO_3 \cdot 0.89\ H_2O$. Infrared spectra of the products were identical to previously published work (*6*). Powder X-ray diffraction data for $MoO_3 \cdot 2H_2O$ could be indexed on the basis of a monoclinic unit cell with a = 7.3581(4) Å, b = 6.918(1) Å, c = 3.7827(5) Å, β = 90.75°, very similar to that reported by Lindquist (*7*). Powder X-ray data for $MoO_3 \cdot H_2O$ were similar to those of Günter (*3*) and could be indexed on the basis of a monoclinic unit cell. Some differences in indexing were noted, however, these being shown in Table I. Guinier-type X-ray cameras and Cu$K\alpha$ radiation were used in both cases. The reflections in Günter's work were broadened (lowering the accuracy) (*3*), which was not the case in this work.

NMR Techniques

The ^1H relaxation times T_2, T_1, and $T_{1\rho}$ were measured in the temperature range

TABLE I

POWDER X-RAY DIFFRACTION PATTERN OF YELLOW $MoO_3 \cdot H_2O$

This work[a]		Günter (*3*)[b]	
d (Å)	$h\ k\ l$	d (Å)	$h\ k\ l$
5.346	0 2 0	5.32	0 2 0
3.539	2 1 0	4.71	$\bar{1}$ 1 1
3.438	0 1 2	3.57	0 0 2
2.936	1 3 1	3.52	2 1 0
2.670	0 4 0	3.41	0 1 2
2.638	$\bar{2}$ 0 2	3.16	0 3 1
2.583	2 3 0	3.00	0 2 2
2.547	0 3 2	2.66	0 4 0
2.374	1 4 1	2.64	$\bar{2}$ 0 2
1.976	1 5 1	2.58	$\bar{2}$ 1 2
1.870	4 0 0	2.52	0 3 2
1.855	2 5 0	2.32	$\bar{3}$ 1 1
1.844	0 5 2	2.09	1 2 3
1.780	0 6 0	2.05	1 4 2
1.768	4 2 0	1.98	3 1 2
1.729	0 6 1	1.84	2 5 0
1.718	0 2 4	1.81	3 4 0
1.688	$\bar{1}$ 6 1	1.78	2 5 1
1.630	$\bar{2}$ 1 4	1.71	0 2 4
		1.65	$\bar{2}$ 5 2
			1 2 4
		1.62	4 0 2

[a] a = 7.492(4) Å, b = 10.679(4) Å, c = 7.282(4) Å; β = 91.1°.

[b] a = 7.55 Å, b = 10.69 Å, c = 7.28 Å; β = 91°.

150–325 K using a Bruker SXP spectrometer, operating at $\omega_0 = 2\pi \times 60$ MHz or $2\pi \times 20$ MHz, and Datalab signal-averaging equipment.

T_2, the spin–spin relaxation time, was measured using the zero-time-resolution technique (*8*), T_2 being taken as the time for the solid echo to decay to $1/e$ of its maximum height, as is done conventionally. The second moments, M_2, were determined from the curvature of the solid echoes at their maxima, a technique of comparable accuracy to continuous-wave methods (*9*).

T_1, the spin–lattice relaxation time, was measured using an inversion-recovery sequence to which a solid-echo read-pulse was added, 180°_x–τ–90°_x–t–90°_y where $t = 17$ μsec. At low temperatures ($T_1 > 3$ sec) a multiple-pulse saturation method, 90°_x–(τ–90°_x–t–90°_y–t–echo–)$_n$, was alternatively used, T_1 being determined from the steady-state amplitude of the echo using the formula

$$M(\tau) = M(\infty)[1 - \exp(-\tau/T_1)]. \quad (1)$$

The two methods gave values agreeing within experimental error.

$T_{1\rho}$, the spin–lattice relaxation time in the rotating frame, was measured using the method of Hartmann and Hahn (*10*) with an additional solid-echo read-pulse. The spin-locking fields, B_1, were determined from the length of 4π pulses on the locking channel to be 37 G for $MoO_3 \cdot 2H_2O$ and 31 G for $MoO_3 \cdot H_2O$. For all $T_{1\rho}$ measurements in this work $\omega_0 = 2\pi \times 60$ MHz.

Results

The temperature dependences of the relaxation times are shown in Figs. 1 and 2 for $MoO_3 \cdot 2H_2O$ and $MoO_3 \cdot H_2O$, respectively. The spin–lattice relaxation times for 60 MHz are denoted T_1^{60} and those at 20 MHz are denoted T_1^{20}.

Corresponding to the slight increase in T_2 on going from low to high temperatures, the observed M_2 values decreased slightly with temperature for both compounds. For $MoO_3 \cdot 2H_2O$, M_2 was 36 G^2 at 165 K and 28 G^2 at 290 K. For $MoO_3 \cdot H_2O$, M_2 was 26 G^2 at 150 K and 24 G^2 at 290 K. Solid-echo maxima were fitted to a form (*11*)

$$g(t) = \exp(-at^2)[\sin(bt)/(bt)] \quad (2)$$

and the standard deviation of M_2 was always ± 1 G^2 or less. M_2 was reproducible within these error limits.

Discussion

The temperature-dependent spin–lattice relaxation behavior in Figs. 2 and 3 shows there to be motion in both these compounds. The low-temperature weak temperature dependence is typical of insulators at such temperatures and results from re-

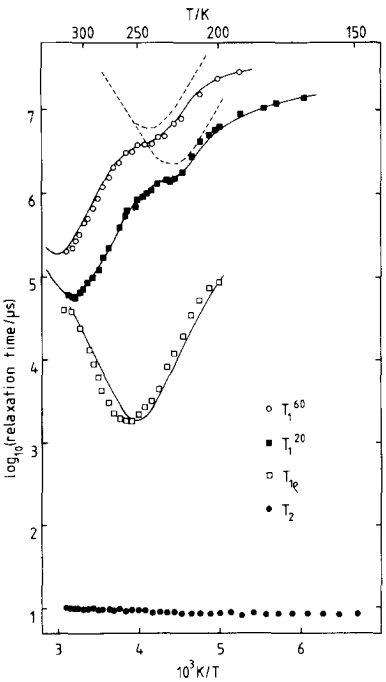

FIG. 2. Temperature dependence of ^{1}H NMR relaxation times for $MoO_3 \cdot 2H_2O$. The solid lines are the theoretical fit to the data (see text). The dashed lines are the calculated contribution T_{1A} from motion A (see text).

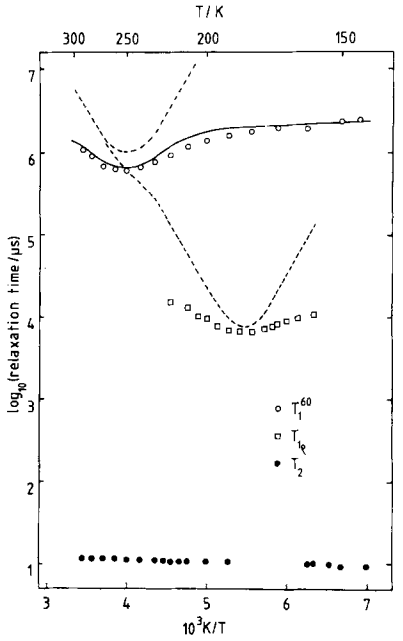

FIG. 3. Temperature dependence of ^{1}H NMR relaxation times for $MoO_3 \cdot H_2O$. The solid line is the theoretical fit to the T_1^{60} data (see text). The dashed lines are the calculated contributions from the flipping motion (see text).

laxation *via* paramagnetic impurities (see e.g. Refs. (*12, 13*)) giving a contribution $1/T_{1\,\mathrm{imp}}$ to the relaxation rate.

The absence of appreciable motional narrowing in T_2 values shows that translation is not being detected and that 180° flips of water molecules about their C_2 axes are occurring. It is well known (see e.g., Ref. (*14*)) that intramolecular dipolar interactions survive this motion while the much smaller intermolecular dipolar interactions are altered.

$MoO_3 \cdot 2H_2O$

Two separate 180°-flipping processes, A and B, are necessary to explain the spin–lattice relaxation behavior of this compound (see Fig. 2). As temperature is increased from 150 K, first motion A is evident in the decrease in the observed T_1 and, at still higher temperatures, a shoulder occurs in T_1 and another decrease, due to motion B, is then seen in T_1. The observed T_1 is given by

$$1/T_1 = 1/T_{1A} + 1/T_{1B} + 1/T_{1\,\mathrm{imp}}, \quad (3)$$

where T_{1A} and T_{1B} are the contributions from motions A and B, respectively. The $T_{1\rho}$ minimum corresponds to the high temperature T_1 minimum (i.e., arises from motion B).

The T_1 and $T_{1\rho}$ data were analysed assuming a BPP-type dependence (see e.g., Ref. (*14*)) of T_{1A} and T_{1B} on τ_r, the correlation time, which was calculated as a function of temperature for motions A and B using computer-generated tables. In the case of motion B, the minimum in T_{1B}^{60} was calculated from the observed minimum in T_{1B}^{20}. Plots of $\log(\tau_r/\mathrm{sec})$ versus $1/T$ gave straight lines, which could imply Arrhenius-type temperature dependences for τ_r's. The values calculated on this basis for τ_r^0's, the preexponential factors, and E_A's, the activation energies, are given in Table II.

The theoretical fits presented in Fig. 2 are calculated from the parameters in Table II. The agreement with experiment is very good.

The calculated minima in T_{1A} (dashed lines in Fig. 2) give the ratio $(T_{1A}^{60})_{\min}$/

TABLE II

REORIENTATIONAL PARAMETERS ASSUMING ARRHENIUS-TYPE TEMPERATURE DEPENDENCES FOR CORRELATION TIMES, τ_r

Compound	Data	τ_r^0 (sec)	E_A (kJ mole^{-1})
$CaSO_4 \cdot 2H_2O$	Ref. (*23*)	2×10^{-14}	26
$LiSO_4 \cdot H_2O$	Ref. (*23*)	1×10^{-15}	31
$MoO_3 \cdot H_2O$	See text	1×10^{-16}	34
$MoO_3 \cdot 2H_2O$	T_{1A}^{60}	7×10^{-16}	29.2 ± 3.3
	T_{1A}^{20}	6×10^{-16}	30.8 ± 2.0
	$T_{1\rho}$	6×10^{-15}	39.0 ± 1.4
	T_{1B}^{60}	1×10^{-15}	39.6 ± 1.0
	T_{1B}^{20}	2×10^{-15}	38.2 ± 0.8

$(T_{1A}^{20})_{min}$ = 2.6 whereas BPP theory predicts 3. The minima used in the calculation are those deduced from the experimental data after subtraction of the contributions from motion B and impurities and are subject to appreciable errors.

$MoO_3 \cdot H_2O$

A single 180°-flipping process is sufficient to explain the relaxation behavior (see Fig. 3). The observed T_1 is given by

$$1/T_1 = 1/T_{1\,\text{flip}} + 1/T_{1\,\text{imp}}. \qquad (4)$$

Assuming an Arrhenius-type temperature dependence for τ_r, values for τ_r° and E_A were calculated from the position of $(T_1)_{min}$ (when $\omega_0\tau_r = 0.616$) and $(T_{1\rho})_{min}$ (when $\omega_1\tau_r = 0.5$) and are given in Table II. These parameters were used to calculate the fit (solid line in Fig. 3) to the T_1 data, which is seen to be good. The predicted contributions $T_{1\,\text{flip}}$ and $T_{1\rho\,\text{flip}}$ (the dashed lines in Fig. 3) are reasonable, especially in the relative positions of $(T_{1\rho})_{min}$ and $(T_{1\rho\,\text{flip}})_{min}$, but there are insufficient data for a detailed fit to $T_{1\rho}$.

Second Moments and Minima

The total observed second moment, M_2, for a hydrate is the sum of intramolecular M_2^{intra} and smaller intermolecular M_2^{inter} contributions. The intramolecular dipolar interaction, giving rise to M_2^{intra}, perturbs the triplet levels of the pair of spin-½ protons, leading to the Pake splitting (*15*) characteristic of hydrates. The triplet state is symmetrical with respect to interchange of the protons, and the splitting (and M_2^{intra}) survives 180° flips of the water molecule. The motion does, however, reduce M_2^{inter}. Pedersen (*16*) has presented a thorough examination of the effects of this motion. In this work the true "rigid lattice" (corresponding to static waters) values of T_2 and M_2 are only observed at the very lowest temperatures. At higher temperatures the 180° flips lead to a small increase in T_2 (and decrease in M_2) due to changes in M_2^{inter}.

The atom coordinates for $MoO_3 \cdot 2H_2O$ given in the literature (*1*, *2*) correspond to M_2 values for the rigid lattice far higher than are observed in this work (36 G² and 26 G² for the di- and monohydrate, respectively) and in hydrates in general. Using van Vleck's formula for powders (*17*), we calculate 103 G² for the coordinates of Asbrink and Brandt (*1*) and 60 G² for those of Krebs (*2*). The M_2 corresponding to isolated H_2O molecules (r = 0.96 Å, Θ = 104.5°) is 29 G². In a hydrate M_2^{intra} can differ from 29 G² by a few G² due to small changes in bond angle Θ and bond length r on insertion into a lattice. M_2^{inter} is typically a few G² or less. The situation is further complicated by molecular vibrations (see e.g. Ref. *14*). The atom coordinates for $MoO_3 \cdot 2H_2O$ (*1*, *2*) give bond lengths and angles (e.g., r = 0.72 °A, Θ = 100°, Ref. (*1*)) which are highly unlikely in view of the known values for hydrates from neutron diffraction and NMR studies (*18–20*). The discrepancy, and the high calculated M_2, is a consequence of refinement of H atom coordinates using X-ray data and does not render the structural model itself incorrect.

The position of a relaxation time minimum is related to the change in M_2 (which in this case is the change in M_2^{inter}) brought about by the motion. In the case of $MoO_3 \cdot 2H_2O$, the position of $(T_{1A})_{min}$ suggests (using BPP theory) a change of 3.1 G² and that of $(T_{1B})_{min}$ a change of 0.1 G². The difference between the sum of these changes and the observed change (≃8 G²) is a consequence of the use of BPP theory and the experimental determination, the change being the difference of two large numbers. For $MoO_3 \cdot H_2O$ the minimum suggests a change of 0.3 G².

The rigid lattice M_2 values (at 77 K) obtained by Maricic and Smith (*4*) (30.7 ± 1.6 G² and 27.6 ± 1.4 G² for the di- and monohydrate respectively) are similar to

those in this work (36 ± 1 G^2 and 26 ± 1 G^2). The small discrepancy in the dihydrate case could be due to different errors in the two determinations. The continuous-wave determination (*4*) had a poorer signal-to-noise ratio than for the monohydrate and any errors in the wings of the spectrum would be very serious. The determination of M_2 from solid echoes may be less accurate than suggested earlier due to error terms which become more serious for shorter T_2 values. By fitting the observed lineshapes (approximately Pake doublets) Maricic and Smith deduced an intramolecular H–H distance of 1.56 Å in both hydrates. Similar M_2 values have been reported for the analogous tungstic acids, $WO_3 \cdot 2H_2O$ (26 G^2 in Ref. (*21*)) and $WO_3 \cdot H_2O$ (25 G^2 in Ref. (*21*) and 27 G^2 in Ref. (*22*)).

Motions and Motional Parameters

Motions A and B in $MoO_3 \cdot 2H_2O$ can be assigned to particular waters on physical and chemical grounds. The interlayer waters participate in three normal hydrogen bonds, which must be broken during a 180° flip. The coordinated waters participate in two normal hydrogen bonds and a bond to an Mo atom, this being shown to be weak by Mo–OH_2 bond length and bond number considerations (*1*). The 180° flipping motion in $MoO_3 \cdot H_2O$ (where all waters are coordinated to Mo) and motion A in $MoO_3 \cdot 2H_2O$ have very similar temperature dependences for τ_r (this being evident in the τ_r^0 and E_A values in Table II). The coordinated waters are chemically very similar in both compounds. Furthermore the change in M_2^{inter} brought about by 180° flips of coordinated waters is expected to be less for the dihydrate as only half the waters are affected. Motion A is therefore reorientation of coordinated OH_2. Motion B is reorientation of interlayer waters and is expected to have a higher activation barrier due to the necessity to interrupt a greater number of H bonds. The interpretation is not complicated by the fact that in $MoO_3 \cdot 2H_2O$ each class of water (interlayer and coordinated) strictly contains four crystallographically inequivalent H_2O molecules (*1*, *2*).

The motional parameters deduced assuming an Arrhenius-type temperature dependence of τ_r can be compared to those found (using the same assumption) for 180° flipping of waters in other crystal hydrates. The parameters calculated from the work of Holcomb and Pedersen (*23*) on gypsum ($CaSO_4 \cdot 2H_2O$) and $LiSO_4 \cdot H_2O$ are given in Table II. The preexponential factors for $LiSO_4 \cdot H_2O$ and motion B (for interlayer waters) in $MoO_3 \cdot 2H_2O$ are similar, but the activation energies are generally higher for the molybdic acids, in which the hydrogen bonds are shorter. High E_A's and short τ_r^0's have been observed for other molecular reorientations. In $(NH_4)_2C_2O_4 \cdot H_2O$, for example, NH_4^+ reorientation occurs with $E_A = 37$ kJ $mole^{-1}$ and $\tau_r^0 = 2 \times 10^{-16}$ sec (very similar to motion A in this work), while 180° flips of H_2O appear to have $E_A = 59$ kJ $mole^{-1}$ in this and the analogous potassium oxalate hydrate (*24*, *25*).

Reorientational attempt frequencies ($1/\tau_r^0$) are expected to be of the order of a typical optical phonon frequency (i.e., $1/\tau_r^0 \sim 10^{12}$–10^{13} Hz) and the preexponential factors deduced so far in this work (and in work on other hydrates) are therefore "anomalously" low. NMR investigations often lead to low preexponential factors. For instance, NH_4^+ reorientation in NH_4Cl occurs with $\tau_r^0 = 2 \times 10^{-16}$ sec (*26*) and the low τ^0's for ion translation in some superionic conductors have been discussed by Boyce and Huberman (*27*). In the latter case, many alternative explanations have been proposed, including a breakdown of absolute rate theory, low dimensionality, and distributions of correlation times arising from several hopping processes. None of these is appropriate here. In this work τ_r values in the restricted range 10^{-5}–10^{-9} sec

are found by applying BPP theory. The apparently linear plot of $\log(\tau_r/\text{sec})$ versus $1/T$ for the experimental data need not imply a linear relationship over a larger range of temperatures and τ_r values. The assumption of an Arrhenius-type behavior for τ_r to evaluate τ_r^0 by extrapolation of the observed "linear" plot may therefore be invalid.

Temperature dependent activation barriers $E_A(T)$ could result from thermal expansion of a sample which leads to changes in the potentials for molecular motions. A single activation energy E_A (Arrhenius behavior) is expected to be strictly valid only at constant sample volume. Frost *et al.* (*28*) investigated molecular reorientation in $(CH_3)_3CCN$ using neutron scattering and, using the assumption of Arrhenius behavior, obtained $\tau_r^0 = 1 \times 10^{-16}$ sec and $E_A = 23.3$ kJ mole^{-1}. They were able to reinterpret their data successfully in terms of a temperature-dependent $E_A(T)$ and physically reasonable preexponential factors $\tau_r^0 \sim 10^{-12}$ sec. The effects of thermal expansion have largely been ignored in previous analyses of NMR data. In the case of the molybdic acids, which have layer structures, thermal expansion is expected to be highly anisotropic.

The correlation time data for $MoO_3 \cdot 2H_2O$ can be reinterpreted in terms of temperature-dependent activation barriers $E_A(T)$ and physically reasonable preexponential factors. τ_r values are unchanged by this and hence the good fit to the NMR relaxation time data remains. τ_r is then given by

$$\tau_r = \tau_r^0 \exp(E_A(T)/RT). \qquad (5)$$

Figure 4 shows the values of $E_A(T)$ calculated assuming $\tau_r^0 = 10^{-12}$ sec for motion of both coordinated and interlayer waters. The temperature dependence of $E_A(T)$ for both processes is seen to be slight (but leads to the apparent Arrhenius behavior observed for τ_r) and the decreases with

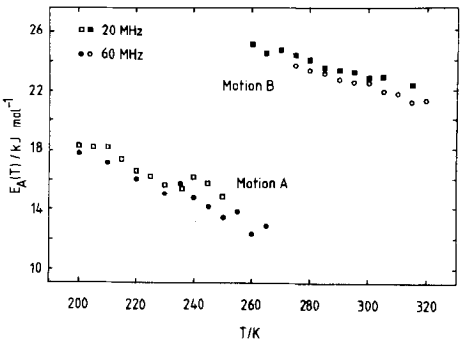

FIG. 4. Temperature dependences of the activation barriers $E_A(T)$ for $MoO_3 \cdot 2H_2O$ assuming $\tau_r^0 = 10^{-12}$ sec for both motion A (of the coordinated waters) and motion B (of the interlayer waters).

temperature could be due to the flattening of potentials on expansion of the unit cell. τ_r^0 should strictly also have a slight temperature dependence.

In the case of the monohydrate there is insufficient data for a plot such as Fig. 4, but a similar interpretation to that above is possible. Assuming $\tau_r^0 = 10^{-12}$ sec, $E_A(T) = 17$ kJ mole^{-1} at 249 K (the T_1 minimum) and $E_A(T) = 20$ kJ mole^{-1} at 183 K (the $T_{1\rho}$ minimum).

Conclusions

NMR relaxation time studies of the molybdic acids, $MoO_3 \cdot 2H_2O$ and yellow $MoO_3 \cdot H_2O$, have allowed investigation of the different temperature dependences of reorientational correlation times for waters coordinated to Mo atoms (in both compounds) and interlayer waters (in the dihydrate). The preexponential factors deduced are physically unreasonable unless temperature-dependent activation barriers are invoked.

The crystalline molybdic acids are hydrates of MoO_3 and no translation of hydrogen atoms has been detected in this work. H atom translation has, however, been found in related compounds which are not simple hydrates. The formally related anti-

monic acid ("$Sb_2O_5 \cdot nH_2O$") is a proton-conducting solid electrolyte due to H atom translation in an H_3O^+/H_2O mix contained in a pyrochlore framework (*13*). The non-stoichiometric hydrogen molybdenum bronze $H_{1.71}MoO_3$ is structurally related to the molybdic acids, being a layer compound containing some coordinated OH_2 groups (*29, 30*) (the framework of the layers is different however). Fast translation of H atoms occurs in the bronze by atom jumps to vacant sites (*30*).

Acknowledgments

We thank the Science Research Council for an Equipment Grant, a Fellowship for RCTS and, in collaboration with RSRE Malvern and Plessey, a CASE award for RHJ.

References

1. S. Asbrink and B. G. Brandt, *Chem. Scripta* **1**, 169 (1971).
2. B. Krebs, *Acta Crystallogr. Sect. B* **28**, 2222 (1972).
3. J. R. Günter, *J. Solid State Chem.* **5**, 354 (1972).
4. S. Maricic and J. A. S. Smith, *J. Chem. Soc. (London)*, 886 (1958).
5. M. L. Freedman, *J. Amer. Chem. Soc.* **81**, 3834 (1959).
6. M. Sotani, Y. Saito, M. Oita, and M. Hasegawa, *Nippon Kagaku Kaishi* **4**, 673 (1974).
7. I. Lindquist, *Acta Chem. Scand.* **4**, 650 (1950).
8. J. G. Powles and J. H. Strange, *Proc. Phys. Soc. (London)* **82**, 6 (1962).
9. P. Mansfield, *Phys. Rev. A* **137**, 961 (1965).
10. S. R. Hartmann and E. L. Hahn, *Phys. Rev.* **128**, 2047 (1962).
11. A. Abragam, "The Principles of Nuclear Magnetism," p. 120. Oxford Univ. Press, London/New York (1961).
12. H. A. Resing and J. K. Thompson, *J. Chem. Phys.* **46**, 2876 (1967).
13. W. A. England and R. C. T. Slade, *Solid State Commun.* **33**, 997 (1980).
14. L. W. Reeves, *Prog. Nucl. Magn. Reson. Spectrosc.* **4**, 193 (1969).
15. G. E. Pake, *J. Chem. Phys.* **16**, 327 (1948).
16. B. Pedersen, *J. Chem. Phys.* **39**, 720 (1963).
17. J. H. van Vleck, *Phys. Rev.* **74**, 1168 (1948).
18. Z. M. El Saffar, *J. Chem. Phys.* **45**, 4643 (1966).
19. Z. M. El Saffar, *Acta Crystallogr. Sect. B* **24**, 1131 (1968).
20. W. C. Hamilton and J. A. Ibers, "Hydrogen Bonding in Solids," p. 212. Benjamin, New York (1968).
21. E. Schwarzmann and O. Glemser, *Z. Anorg. Allg. Chemie* **312**, 45 (1961).
22. V. Ya. Kabanov and V. F. Chuvaev, *Russ. J. Phys. Chem.* **38**, 717 (1964).
23. D. F. Holcomb and B. Pedersen, *J. Chem. Phys.* **36**, 3270 (1962).
24. T. Chiba, *Bull. Chem. Soc. Japan*, **43**, 1939 (1970).
25. J. W. McGrath and A. A. Paine, *J. Chem. Phys.* **41**, 3551 (1964).
26. T. Kodama, *J. Magn. Reson.* **7**, 137 (1972).
27. J. B. Boyce and H. A. Huberman, *Phys. Rep.* **51**, 189 (1979).
28. J. C. Frost, A. J. Leadbetter, and R. M. Richardson, *Faraday Discuss. Chem. Soc.* **69**, 32 (1980).
29. P. G. Dickens, J. J. Birtill, and C. J. Wright, *J. Solid State Chem.* **28**, 185 (1979).
30. R. C. T. Slade, T. K. Halstead, and P. G. Dickens, *J. Solid State Chem.* **34**, 183 (1980).